Chapter 6

Engineered Polyurethane with Glycine and its homopeptides: A biomimetic approach for targeted drug delivery in cancer therapy

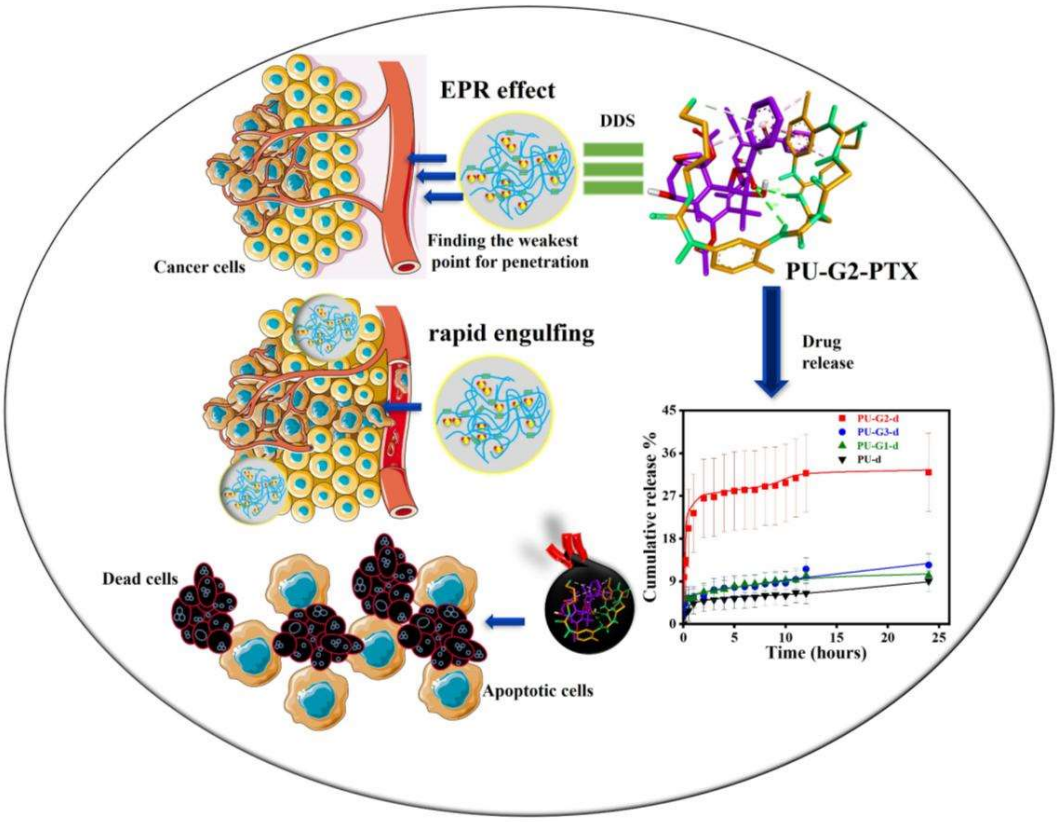

Chapter 6

6.1 Introduction

Targeted therapy is achieved by directly exploiting the unique molecular markers or genetic mutations present in the cancerous cells. Unlike traditional chemotherapy, which causes killing of healthy cells in addition to cancer cells. It would be called, in this context of targeting cancer with therapeutic agents through a mechanism called the "Blitzkrieg or lightning war," a type of delivery strategy where direct introduction into the cancer cells is brought about by employing the mechanisms of the cellular system themselves to internalize foreign structures within its system more like exploiting the EPR effect of cancer cells. The term "Blitzkrieg" is used because, similar to the military strategy developed by Germany during World War II, which emphasizes a “rapid”, "focused approach to overwhelm a specific target" for achieving swift victories, i.e., leading to the delivery of the therapeutic payload. An example of this is RGD[109] for improved cancer treatment or internal cancer uses. Short amino acid sequences known as RGD (arginine-glycine-aspartic acid) peptides have demonstrated significant promise in the therapy of cancer because of their capacity to target integrins. Integrins are cell surface receptors that are often overexpressed in cancer cells as well as the vasculature surrounding tumors. Integrins are crucial for adhesion, migration, and survival of cells. For the "next generation" DDS-based systems with superior efficacy, peptides mimicking ECM components, such as those containing the RGD surface or integrin-binding sequence and characteristics, should be added to attain better treatment of cancer therapy. Henceforth, we have synthesized polyurethane using aromatic diisocyanates, Gly, and its homopeptides (as chain extenders) to increase the selectivity and sensitivity as drug delivery systems. Gly is the smallest and simplest amino acid, whose homopeptides we have

used for providing an RGD-like matrix for the current study. The findings have been discussed in section 6.2.

6.2 Results and Discussion

6.2.1 NMR Analysis

The reaction involved modifying the hydrophilicity and architecture of PU by varying the extent of grafting onto polyurethane. This process involved reacting isocyanate-terminated prepolymer, followed by linking the chain extender (Gly, Gly-Gly, Gly-Gly-Gly, respectively) through amine groups, resulting in a branched structure. Confirmation of the grafting was achieved through ^{1}H NMR spectroscopy, as depicted in **Figure 6.2** and supported by FTIR and UV-VIS spectroscopy, **Figure 6.2.2.1a** and **b,** respectively.

Typical singlet peaks of -CH_2 unit are visible in the spectra at 5.78 (e, PU-G1), 5.77 and 5.29 (e, f, PU-G2), and 5.78, 5.31, 5.17 ppm (e, f, n, PU-G3). The identical peak in glycine or peptides can be found between 3.4–4.4 ppm[260,261]. The proton in urethane -NH-COO linkages causes it to peak at 8.28 ppm (PU, c)[169], but in the grafted ones, it exhibits 9.42–9.44 ppm[175,262] . The Ph–CH3 group of TDI appears at 2.66 (singlet, d)[263] ppm in every moiety. Two triplets at 4.88 (a) ppm and 4.61 (b) ppm come from the (-O-$^{a}CH_2$-$^{b}CH_2$-$^{b}CH_2$-$^{a}CH_2$-O-) group of PTMG, found in all the samples. Lastly, multiplets at 6.54–7.04 in PU[169] and 6.39–7.43[171] ppm in grafted PUs is responsible for the aromatic protons[262], along with those different types of -NH- protons ranging from 7.78–9.44 ppm[177,264] are found in grafted PUs, confirming the reaction between prepolymer and chain extenders.

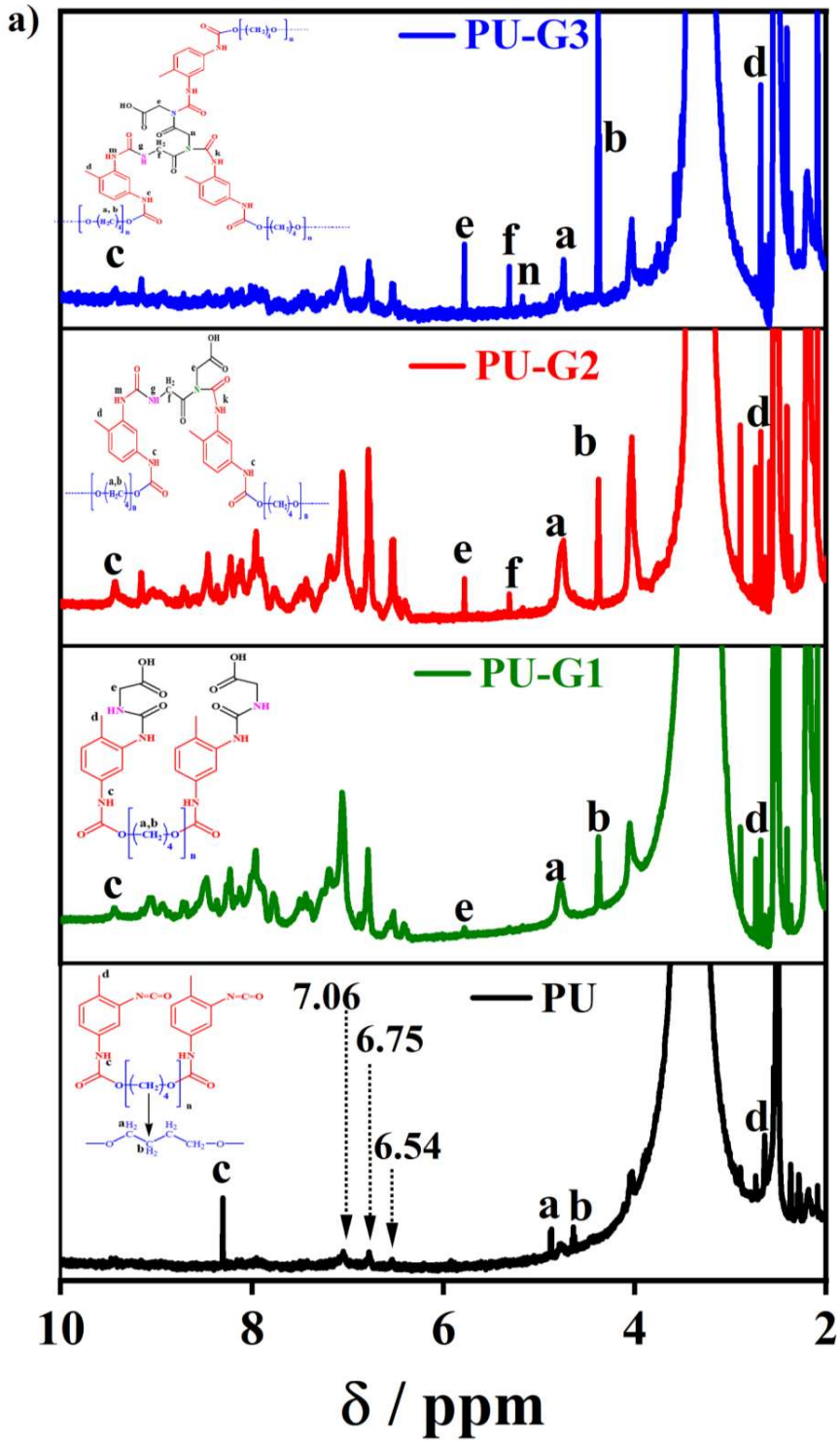

Figure 6.2: ^{1}H NMR of all the samples (pure PU, PU-G1, PU-G2, and PU-G3) is represented with the corresponding peaks labeled as “a” and “b” etc.

6.2.2 Spectroscopic characterization in correlation with crystallinity and structural aspect

The structural variations between synthetic polyurethane's hard and soft segments were examined using FTIR spectroscopy (**Figure 6.2.2.1a**). **Table 6.2.2** compares and tabulates the variations in experimental FTIR spectra between grafted and pure PU.

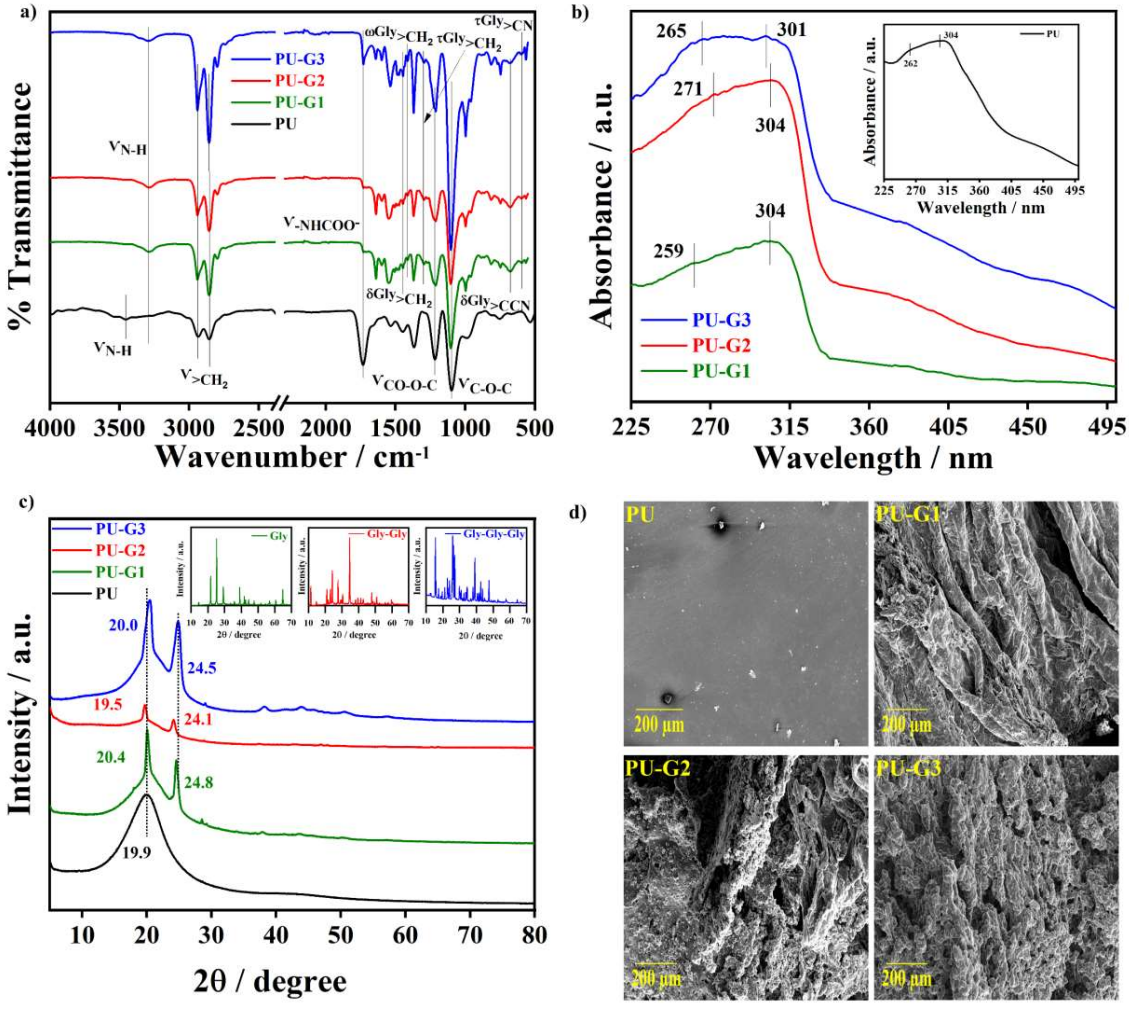

Figure 6.2.2.1: a) FTIR spectra of all the polymers display shifts in peak positions resulting from interactions, and the corresponding values are tabulated in Table 1, b) UV–VIS spectra showing peak positions for the $\pi \rightarrow \pi^*$, $n \rightarrow \pi^*$ transition of the carbonyl peak and marked by vertical lines, c) XRD patterns of all polymers, highlighting their crystallinity, d) SEM images to show the morphology of various PU samples.

Table 6.2.2: IR vibrational assignments

Spectral region in IR (cm^{-1})	PU (cm^{-1})	PU-G1 (cm^{-1})	PU-G2 (cm^{-1})	PU-G3 (cm^{-1})	Reported Values (cm^{-1}) with ref
^{V}N-H	3394	3286	3287	3292	(3500-3200)[265]
>CH_2 (anti-symmetrical and symmetrical stretching)	2934 2855	2941 2856	2940 2857	2940 2856	2950[126] 2870
02-^{V}NHCOO-	1732	1729	1729	1730	1730[265]
-^{V}NHCOO- (H-bonded CO)	1662	1639	1639	1641	(1643–1620)[266]
-^{V}NH- deformation	1601	1598	1598	1599	(1595-1574)[130,131]
-^{V}NH- bending	1536	1548	1548	1537	(1533-1524)[267]
^{V}C=C (benzene)	1441	1505	1505	1489	(1488-1474)[267]
$^{\delta}$>CH_2	—	1446	1446	1446	1445[268]
$^{\omega}$>CH_2	—	1413	1413	1413	1413[268]
$^{\tau}$>CH_2	—	1295	1295	1295	1312[268]
^{V}CO-O-C	1217	1211	1210	1210	1240[126]
^{V}C-O-C	1099	1103	1103	1103	1097[269]
$^{\delta}$>CCN	—	679	676	676	699[268]

$^{\tau}$ >CN	—	594	596	596	598[268]

Each of these values has a strong correlation with the literature that has been reported. **Figure 6.2.2.2a** displays the FTIR spectra for each of the chain extenders (Gly, Gly-Gly, and Gly-Gly-Gly). All compounds in the range 200-400 nm had their UV−VIS spectra analyzed (all chain extender's UV-VIS spectra are shown in **Figure 6.2.2.2b**). All polymers displayed noticeable absorption bands at 262-271 nm, attributed to $\pi - \pi^*$ transitions[229]. The peak due to $n-\pi^*$ transition is at (301-304) nm. As glycine moiety is the most basic amino acid without a double bond, there is no discernible change in the UV-VIS spectra following its addition, as seen in **Figure 6.2.2.1b**. The most important method for determining the kind of crystallization is XRD. When the XRD spectrum for the current investigation was taken, pure PU showed a single diffuse peak at about[270] $2\theta=19.9^{\circ}$, suggesting a particular degree of crystallinity that most likely originated from the crystalline nature of PTMG, which is still identifiable inside the PU lattice after polymerization. However, the grafted ones are semicrystalline (as seen in **Figure 6.2.2.1c,** distinct minute peaks occur that are due to Gly moiety), when chain extenders are inserted into the PU matrix, somehow enhancing the crystallinity. These results are aligned with previous literature reports[231,232,271–274]. Pure PU shows a homogeneous sheet-like structure because of its stiff segments and strong intermolecular interactions (**Figure 6.2.2.1d**)[141,266]. The morphology is altered dramatically when Gly/peptides are added as a chain extender. The ordered arrangement of the polymer chains may be upset by the flexible peptide, resulting in the creation of a more asymmetrical and porous structure. This modification can improve the material's permeability and flexibility, which makes it appropriate for use in drug administration, where a more complex morphology can help the material interact with biological systems and save the drug from

degradation in physiological conditions. As cancer upsets the balanced microenvironment of cell by triggering abnormal remodelling of the ECM. These ECM changes have the ability to affect gene expression, facilitate uncontrollable growth, and facilitate increased cell migration, eventually leading to cancer progression and malignancy[275]. Pathways like Ras-Raf-MEK-ERK are instrumental in controlling such events. In a similar vein, PU-

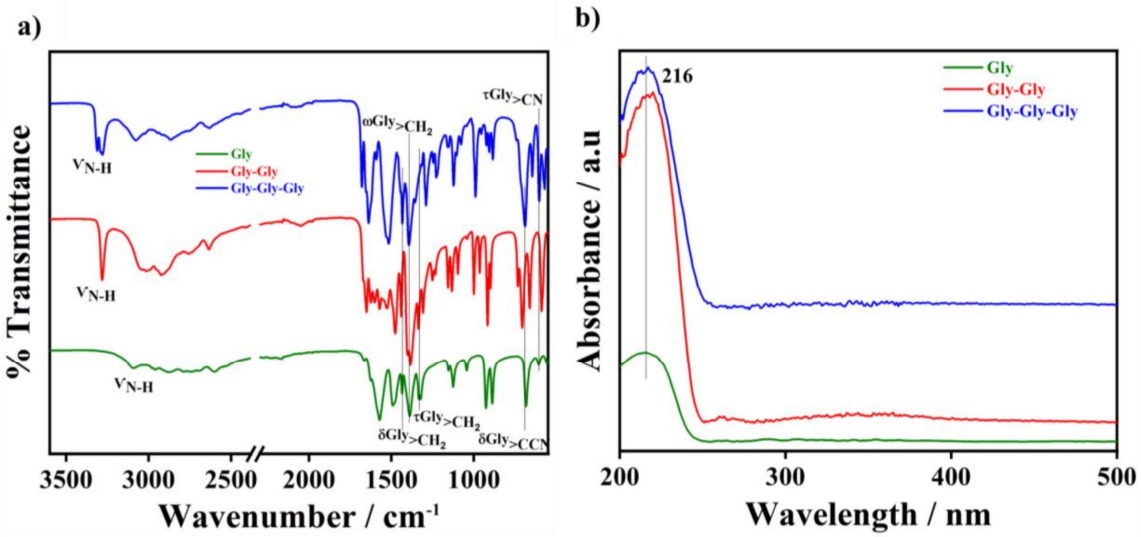

Figure 6.2.2.2: a) FTIR and b) UV-Visible spectra of Pure Gly, Gly-Gly, Gly-Gly-Gly.

Gly systems may control cell fate and proliferation[276] of mesenchymal stem cells[277–279] through affecting mechanotransduction[280,281]. With biological signals, such as polymeric systems, that interact with the cells and ECM to restore or sustain the microenvironmental[282] homeostasis[283].

6.2.3 Thermal behavior

The differential heat of fusion for PU-G1, PU-G2, and PU-G3 is 21.3, 17.1, and 15.8 J/g, respectively, compared to 5.7 J/g for pure PU, indicating significant crystallization (**Fig. 6.2.3a**). PTMG unit is not enough crystalline as seen by the lower melting of pure PU. The

lower value of ΔH in the case of PU-G3 is most likely owing to greater component interaction (two independent components can lay on top of each other), but the higher T_m is related to enhanced crystallization of a larger number of polyurethane units (PU-G3). Polymers with crosslinking, chain rigidity, or the incorporation of bulky side groups can raise the melting temperature by making it more difficult for the polymer chains to move and transition to a

disordered state. However, these same factors might reduce the amount of energy required to break the inter-chain forces, leading to a lower heat of fusion. Because of their length, PU-G3 gives the polymer matrix considerable stiffness and bulk, which helps strengthen the polyurethane's overall structural integrity.

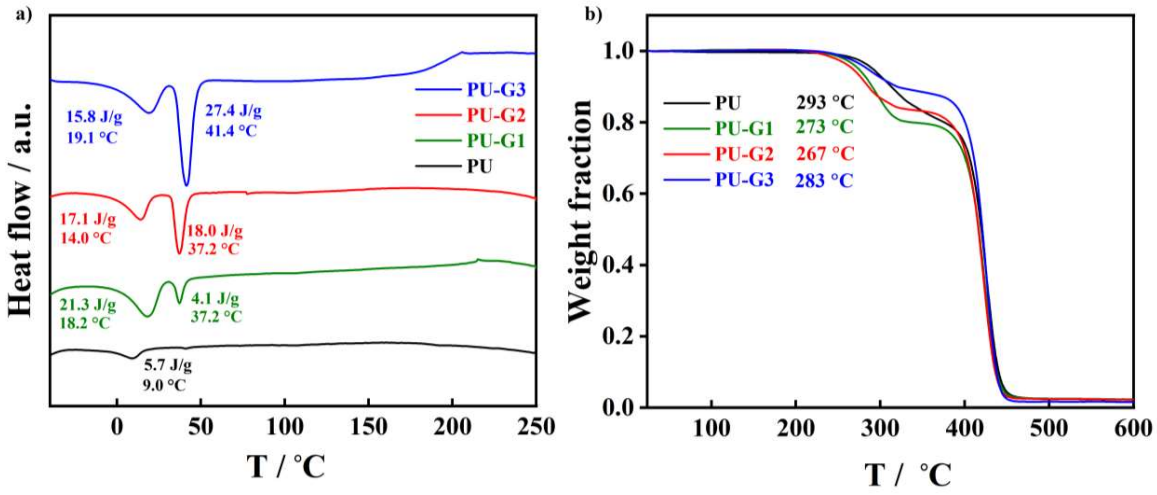

Figure 6.2.3: a) DSC thermograms of all PU samples are shown, with melting temperatures and heat of fusions indicated in the corresponding color codes, b) Thermal stability (TGA thermograms) of all samples as measured through a thermogravimetric analyzer.

The mobility of polymer chains during melting may be hampered by this larger structure, which boosts the second melting and heat of fusion. G2/G3 have more functional groups (e.g., -NH_2 and -COOH) along their chain, which increases hydrogen bonding compared to single amino acid (G1). These hydrogen bonds can strengthen the connections between the

tripeptide segments and the polyurethane matrix. As a result, the tripeptides may increase the crystallinity or semi-crystallinity of the polyurethane, resulting in a higher second heat of fusion and melting temperature.

Thermal stability of all the samples was evaluated by TGA (**Figure 6.2.3b**). The temperature at which the sample started to lose 5% of its weight under an inert atmosphere was used to calculate the thermal degradation. Across all the PU samples, no significant deterioration has been seen below 260 ºC temperature, all specimens exhibited two-step degradation (as seen in the DTG graph in **Figure 6.2.3.1**).

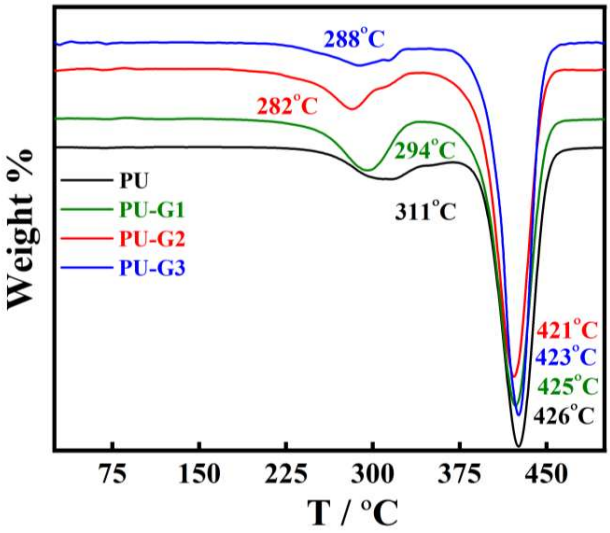

Figure 6.2.3.1: represents the DTG graph showing the degradation temperature of both polymers.

The degradation temperatures are found to be 293 ºC for PU and decrease on going from PU-G1 (273 ºC) to PU-G2 (267 ºC), except for PU-G3 (283 ºC), probably because of the better shielding of heat because of the bulky structure of G3. Thermal degradation of PU is caused

by a breakage of chemical bonds within the macromolecular chains. First, there is a urethane bond breakage, which is followed by a polyol breakdown. The thermal stability of the urethane linkage degradation temperature (in PU) is largely unaffected by the inclusion of hard segments [264,284].

6.2.4 Sustained reléase of drug using varying PU structure

The process by which drugs move from their original location within a polymer matrix to the surrounding medium is referred to as drug release from polymeric systems. The formula ($M_t/M_\infty = kt^n$)[204] is frequently used to study drug release vs time curves to gain more about how drugs are released from polymeric matrixes. The expression for the release rate is a function of time (t), and the diffusional exponent (n) in this equation represents the drug's mode of transport through the matrix, where $0.5 < n < 1$ implies non-Fickian diffusion and $n = 1$ suggests a zero-order release, and k is constant, associated with the matrix system's properties). **Figure 6.2.4. (i)a** depicts a cumulative release (up to 7 days) of PTX over time from both pure PU and grafted PUs in PBS solution. Within 24 hours, PU-G2 releases (maximum) 31% of the implanted drug compared to 9% for pure PU. The release pattern of PTX in PBS buffer over time shows a consistent and prolonged release from all the systems, most likely as a result of stronger H-bonding interactions between drug and polymer, as demonstrated by the molecular docking structures displayed in **Figure 6.2.4. (ii),** and the corresponding values are provided in **Table 6.2.4.2**. Kinetic parameters (in **Figure 6.2.4. (i)c** and values represented in **Table 6.2.4.1**) reveal that all the systems follow Higuchi model, while PU-G3 uses both first-order kinetics and KP model of diffusion. First-order kinetics, in which the rate of release is proportionate to the concentration of drug left in the polymer matrix, may apply to the first burst release. A transition to a KP model, in which the release

rate is determined by a power law that can explain erosion and diffusion processes, may occur when the drug concentration falls. In formulations, especially those incorporating biodegradable or swelling polymers, where distinct processes predominate at different times, combining these kinetics is frequent. Depending on the state of the system, a combination of the two models may be used to describe the total release profile.

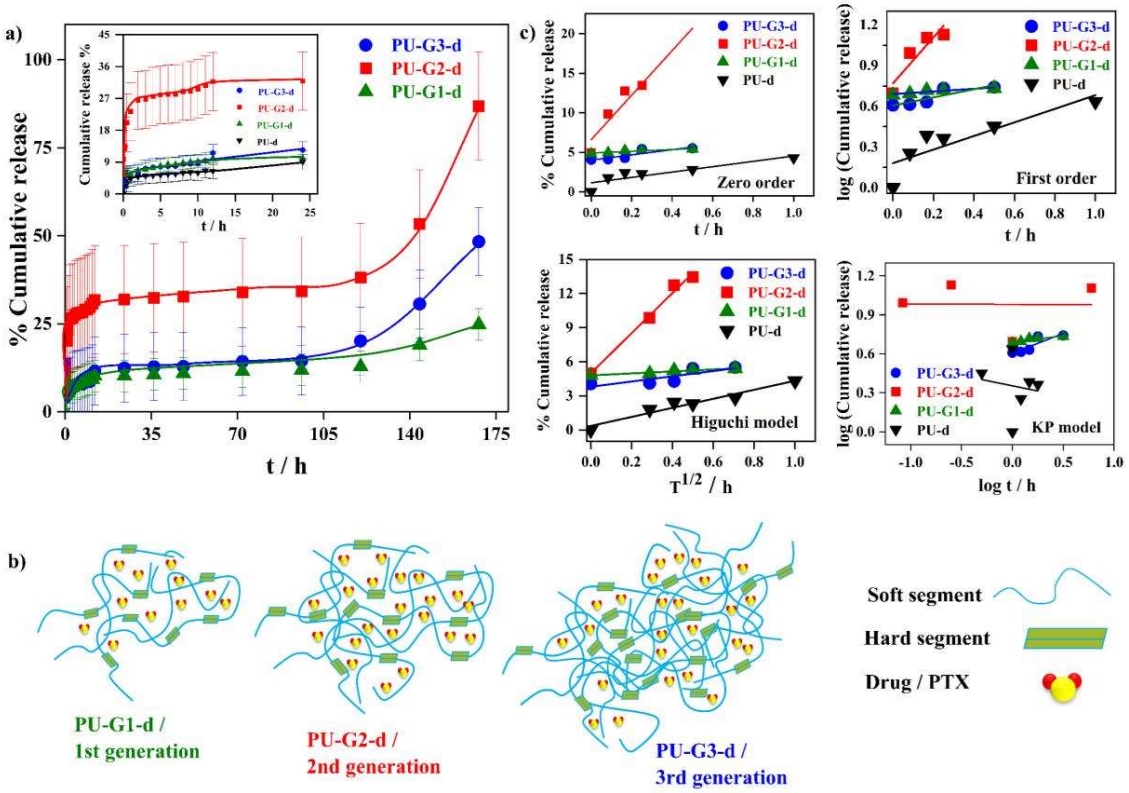

Figure 6.2.4. (i): a) Cumulative drug release from the specimens demonstrates a sustained release profile from the polymers, b) Diagram illustrating the PU's design filled with the drug that results in a prolonged release, c) Drug release profiles of all of the specimens including Zero-order, First order, Higuchi model and KP model in a, b, c and d respectively.

Therefore, although a polymer can essentially follow one paradigm, in certain situations it can also display behavior typical of the other. Swelling increased with hydrophilic (amino-

Table 6.2.4.1: represents the kinetics parameter of drug release

Compositions	Zero Order	First Order	Higuchi Model	KP Model
PU-d	Intercept=1.2± 0.4 Slope=3.44 ± 0.8 r^2 =0.78	Intercept=0.18± 0.06 Slope=0.50 ± 0.14 r^2 =0.75	Intercept=0.4 ± 0.27 Slope=3.9 ± 0.47 r^2 =0.94	Intercept=0.35 ± 0.09 Slope=-0.16 ± 0.5 r^2 =0.02
PU-G1-d	Intercept=4.9 ± 0.07 Slope=1.13 ± 0.3 r^2 =0.83	Intercept=0.7 ± 0.06 Slope=0.09 ± 0.02 r^2 =0.82	Intercept=4.8 ± 0.06 Slope=0.88 ± 0.14 r^2 =0.93	Intercept=0.69 ± 0.06 Slope=0.09 ± 0.02 r^2 =0.83
PU-G2-d	Intercept=6.0 ± 1.2 Slope=34.0 ± 7.9 r^2 =0.90	Intercept=0.77 ± 0.08 Slope=1.7 ± 0.5 r^2 =0.84	Intercept=4.9 ± 0.5 Slope=17.6 ± 1.3 r^2 =0.98	Intercept=0.9± 0.13 Slope= -0.003± 0.17 r^2 =1.93549E-4
PU-G3-d	Intercept=4.0 ± 0.27 Slope=3.3 ± 1.02 r^2 =0.77	Intercept=0.6± 0.02 Slope=0.3 ± 0.09 r^2 =0.78	Intercept=3.8 ± 0.38 Slope=2.3 ± 0.87 r^2 =0.70	Intercept=0.6± 0.02 Slope=0.3 ± 0.09 r^2 =0.78

acid/peptide) content, shifting the drug release mechanism from Fickian diffusion to non-Fickian diffusion. Additionally, the grafted PU's -COOH groups, which interact with PTX's –NH and -OH groups, sped up the rate of drug release. A comparison of the drug release rate at 37 °C in PBS (pH 7.4) revealed the following order: PU<PU-G1<PU-G3<PU-G2. Presumably, because the hydrophobic drug is more palatable to the media due to its bioactive, tiny hydrophilic counterparts[208]. When a hard segment with hydrophilic nature is added, the water uptake rate of the PU with the hydrophobic soft segment (PTMG) increases. PU's network porosity affects the rate at which entrapped pharmaceuticals are released and the of drug diffusivity hydration/water absorption. Mobility increases as a result of the

absorbed water molecules creating water channels inside the polymer network, that allow the drug molecules to exit out of the matrix. One important fact to note is that tripeptide-based polyurethanes/PU-G3 typically show slower release profiles compared to dipeptide-based polyurethanes/PU-G2 due to their more complex structure. The presence of an additional amino acid in the tripeptide sequence increases the molecular weight and potential for intramolecular interactions, such as hydrogen bonding. These interactions can lead to a more robust and less permeable polymer network, thereby slowing down the release of encapsulated drugs. Additionally, the degradation of PU-G3 may also be slower due to the increased steric hindrance[285,286] and the potential for more stable secondary structures, further contributing to a slower release rate. The slower release of PU-G3 can also be explained by the molecular docking interactions. Molecular docking experiments revealed that paclitaxel can interact with PU-G1, PU-G2, and PU-G3 systems based on binding energy {**Figure 6.2.4(ii)**}. **Table 6.2.4.2** shows that paclitaxel exhibited binding affinity to all grafted systems, with binding energies of -5.5 (PU-G1), -5.0 (PU-G2), and -4.5 (PU-G3) kcal/mol[287]. PU and all other polymers interact with the residues of PTX via[205,206] (-CONH-PU, -COO-PTX), (-COO-PU, -OH-PTX), (-CONH-PU, -OH-PTX), (-OH-Gly, -COPh-PTX), (-NH-TDI, COPh-PTX), and (-NH-TDI, -OH-PTX), (-O-PTMG, -OH-PTX), (-CONH-TDI, -OH-PTX). Possible interactions between pure PU and paclitaxel were also investigated, with binding energies and other interaction values given as well**.** Strong molecular interactions (like hydrogen bonding or van der Waals forces) with the drug can create a stable complex. Nonetheless, the drug may still be released quickly if the polymer matrix is similarly permeable. Another factor that may be important is the polymer chain's flexibility.

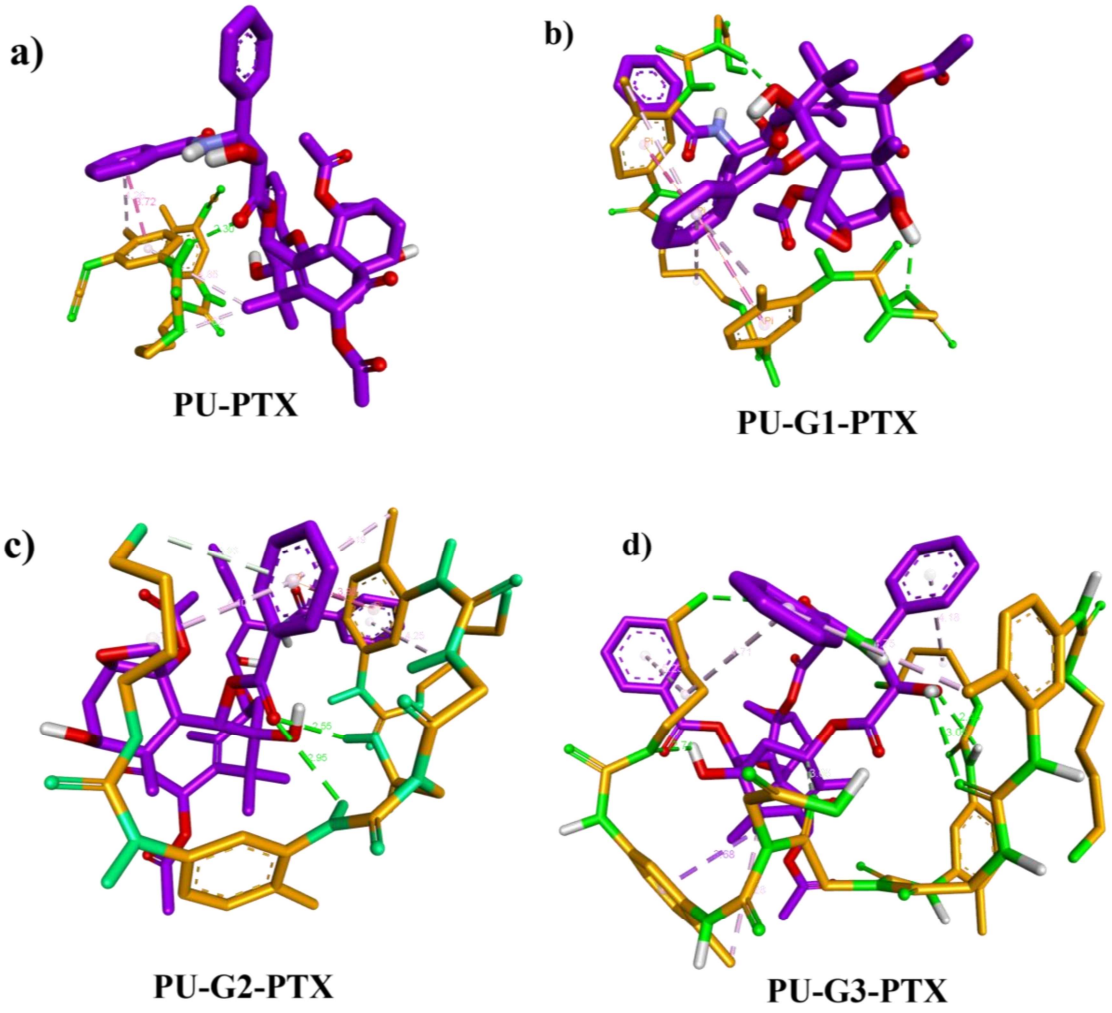

Figure 6.2.4.(ii): Drug-polymer interactions images **a)** PU-G1, b) PU-G2, c) PU-G3, d) pure PU.

A dipeptide structure may be more flexible than a tripeptide structure, which could result in quicker drug delivery. Increased H-bonding may result in a more stable contact between the drug and the polymer matrix, but if these interactions are too strong, the drug may be effectively "trapped" inside, slowing its release. Possibly due to the extra amino-acid unit in tripeptide, the polymer structure may become more rigid or tight, which would decrease chain mobility, and, as a result, the diffusion rate would slow down. This may be the reason for the slower release of PU-G3, where the molecule forms a stable complex with PTX and

protects it from further degradation in biological conditions, but the complex is too strong to release drug at the site of action as well.

Table 6.2.4.2: shows the molecular interaction values between drug and grafted polymers

Ligand-receptor complex compound	Docking score (kcal/mol)	Type of bonds	Bond distance (Å) & interacting residues
PU-G1	**-5.5**	**2** H-bonds **2** pi-pi **3** pi-alkyl	**2.16** (-COO-PU, -OH-PTX); **2.42** (-CONH-PU, -OH-PTX) **3.83** (-Ph-TDI, -Ph-PTX); **4.15** (-Ph-TDI, -Ph-PTX) **4.0** (-CH_3-TDI, -Ph-PTX); **4.88** (-CH_3-TDI, -Ph-PTX); **5.32** (-CH_2-PTMG, -Ph-PTX);
PU-G2	**-5.0**	**2** H-bonds **1** pi-pi **3** pi-alkyl	**2.55** (-OH-Gly, -COPh-PTX); **2.95** (-NH-TDI, -COPh-PTX) **3.88** (-Ph-TDI, -Ph-PTX) **3.93** (-OCH_2-PTMG, -Ph-PTX); **4.10** (-CH_2-PTMG, -Ph-PTX); **4.19** (-CH_3-TDI, -Ph-PTX)

PU-G3	**-4.5**	**4** H-bonds	**2.43** (-NH-TDI, -OH-PTX); **2.71** (-O-PTMG, -OH-PTX); **3.05** (-CONH-TDI, -OH-PTX); **3.32** (-O-PTMG, -NH-PTX)
		5 pi-alkyl	**3.68** (-Ph-TDI, -CH_3-PTX); **4.18** (-CH_2-PTMG, -Ph-PTX); **4.71** (-CH_2-PTMG, -Ph-PTX); **4.75** (-CH_3-PTMG, -Ph-PTX); **5.23** (-CH_2-PTMG, -Ph-PTX)
		2 alkyl-alkyl	**3.66** (-CO-Gly, -CH-PTX); **4.28** (-CH_3-TDI, -CH_3-PTX)

Meanwhile, in the case of pure PU and PU-G1 hydrophobicity primarily plays the major role in lowering the drug release whereas in the case of PU-G3 although hydrophilicity increases the structural rigidity and more no of interaction with drugs retards the release from the matrix. In PU-G2 both the factors become moderate and it stands out as the best among all the three. The pure PU-PTX interaction is already shown in Chapter 4 (**Table 4.2.4.2**).

6.2.5 Biocompatibility and *in-vitro* treatment efficacy

Biomaterials and, drug carrier systems need to be biocompatible and non-cytotoxic in and of themselves. Therefore, a biocompatible material ideally fulfills its intended purpose without having any negative local or systemic impacts. Phase-contrast images of 3T3 and SiHA cells cultured on the material bed were taken in order to evaluate the cytotoxicity of the polymer structure via cell adhesion. This showed enhanced cell adhesion on the polymer

structure as evidenced by the well-spread morphology (**Figure 6.2.5.1a** for SiHA and **b** for 3T3). Since the 3T3 cell line has a length of (50-100) µm and SiHA has a length of (20-50) µm, the images of the 3T3 cell line were taken at 20x resolution, while the images of SiHA were obtained at 40x resolution to obtain a clearer cell morphology. But occasionally, the length fluctuates according to the type of material bed we're employing. OD value demonstrates that grafted PU exhibits more biocompatibility over pure PU, probably because of the amino-acid/peptide counterpart in the moiety. Compared to healthy cells, the OD values of the cellular assessment data (**Figure 6.2.5.1c** for SiHA and **d** for 3T3 cells after 24 hours) show improved adherence of material to cancer cells. This finding may improve targeted delivery of anticancer drugs. Cell type, ambient conditions, surface physicochemical characteristics, and other factors all play a role in the intricate process of cell adhesion. Proteins that cells release and the cell adhesion receptors (mainly, integrins)[288], allow them to connect with the surface indirectly instead of directly. The morphology of polyurethane grafted with peptides may be more conducive to cancer cell adhesion, in contrast to normal cells, as cancer cells are better at modifying their mechanical properties [289]. According to SEM images [290] the crystalline and amorphous regions in some ways, ideally suited for this type of adherence as the surface gets rougher. Peptide modifications may mimic components of the extracellular matrix (ECM), such as integrin-binding sequences like RGD (Arg-Gly-Asp)[291], which are known to promote cell adhesion.

Cancer cells tend to express a higher number of integrins (during metastasis), allowing them to adhere more effectively to surfaces that present these sequences. The peptide modification on polyurethane may simulate this environment, making it more favorable for SiHA cells to adhere and grow. This difference in integrin profiles could lead to stronger interactions

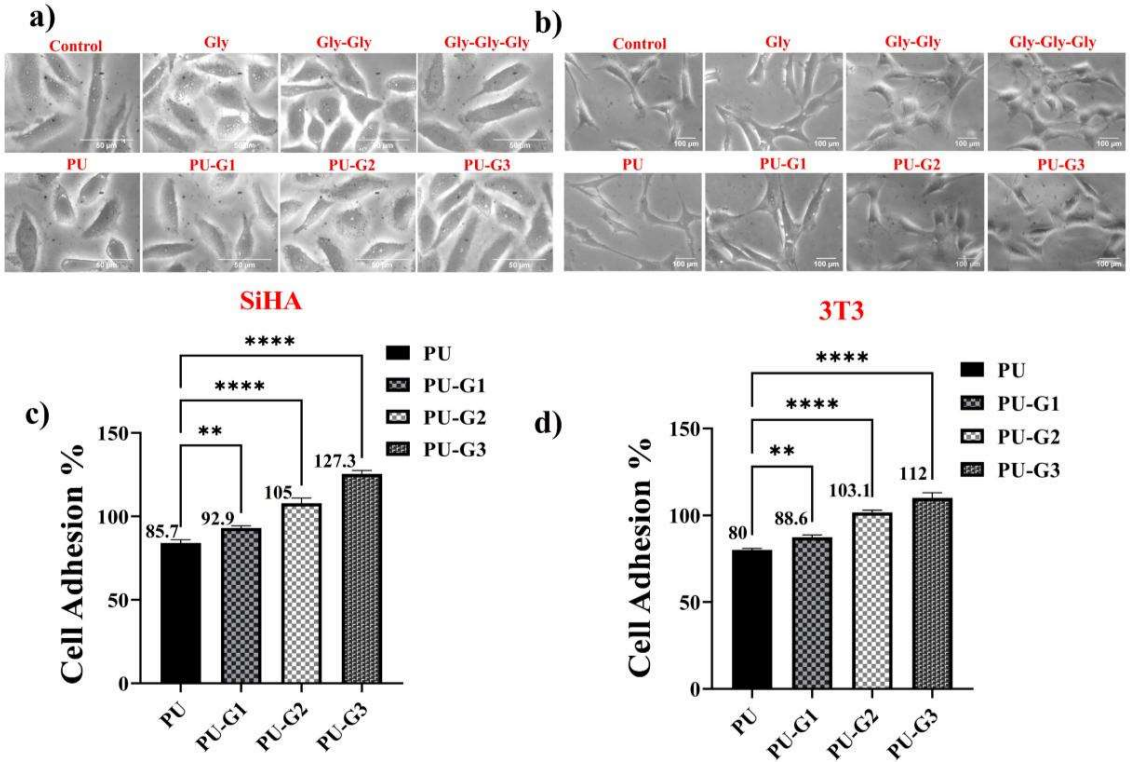

Figure 6.2.5.1: Biological responses of all the polymers assessed through cellular studies, a) Morphology of SiHA cells cultured on pure PU and grafted PU surfaces, captured by microscopy with a gray filter after one day of sample proliferation (cell adhesion magnification = 40×), b) Evaluation of cell adhesion using optical density profile data for adhered SiHA cells across the sample bed, c) Morphology of SiHA cells cultured on pure PU and grafted PU surfaces, captured by microscopy with a gray filter after one day of sample proliferation (cell adhesion magnification = 20×), d) Evaluation of cell adhesion using optical density profile data for adhered 3T3 cells across the sample bed.

between cancer cells and peptide-grafted polyurethane, especially if the peptides are tailored to bind specific integrins. Three days of MTT assays with concentrations ranging from 20 to 100 µg/ml were conducted on 3T3 and SiHA cell lines in order to determine which one among the three grafted PUs was the best and the data made it clear that all the grafted PU shows more than 90% biocompatibility in both cell lines (at 20 µg/ml). **Figure 6.2.5.2**(**a** for 3T3, and **c** for SiHA) contains corresponding OD values for 20 µg/ml, which is as per the literature reports. The grafted PUs display above 75% cell viability (for PU-G2 and PU-G3)

at 100 µg/ml as well, after 3rd day of study (**Figure 6.2.5.2b** for 3T3 and **d** for SiHA). Thus, chain extenders improve the PU system's biocompatibility and bioavailability to tumor cells, making it one of the most efficient drug delivery carriers in real-world applications.

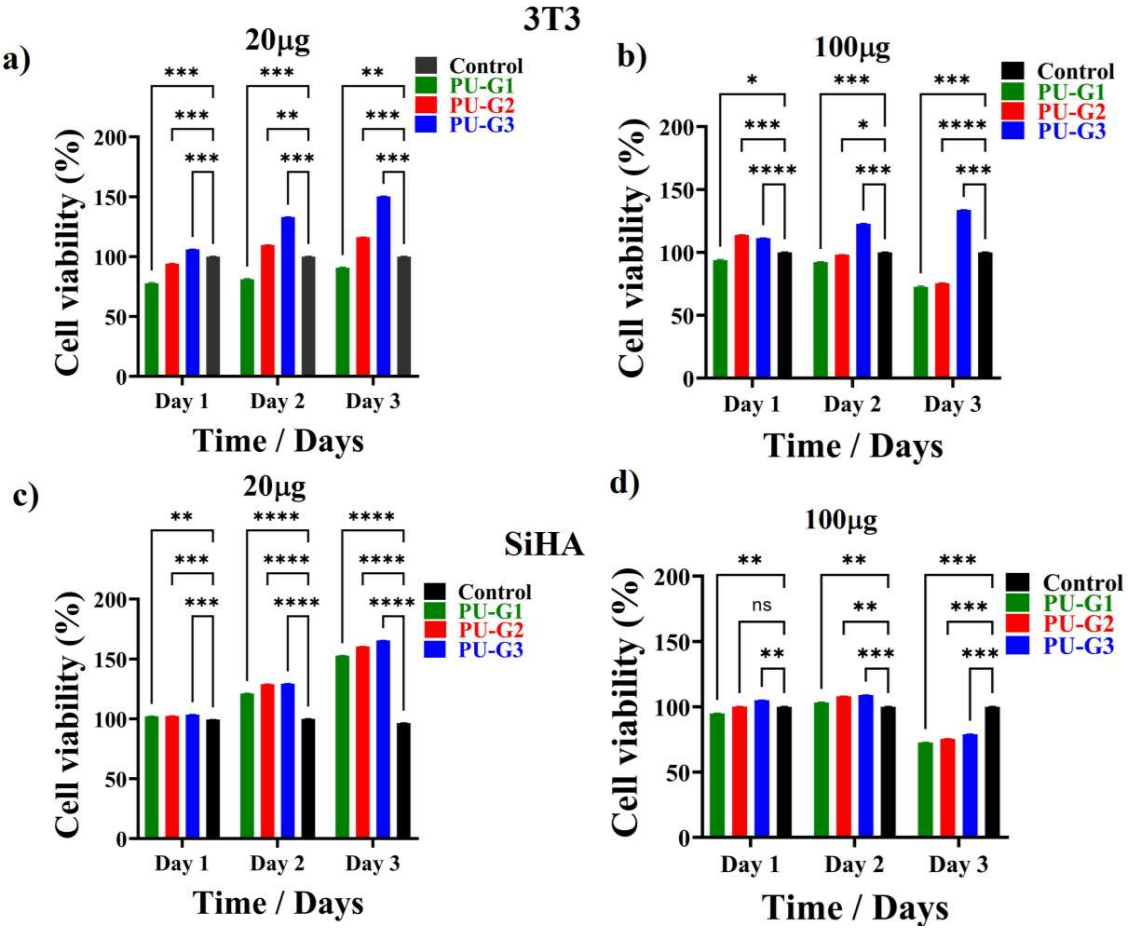

Figure 6.2.5.2:shows the biocompatibility of all the samples via MTT data in both SiHA and 3T3 cell lines, ranging from (20 to 100) µg concentration

The dose-dependent results of cell viability study are presented in **Figure 6.2.5.3 (a, b).** The cultured 3T3 cell line exhibited consistent viability across all tested PUs. Notably, even at a concentration of 100 µg/ml, a high level of cell viability was maintained, with over 90% of

the cells (for PU-G2-d and PU-G3-d) remaining viable throughout the 72-hour study period (**Figure 6.2.5.4a** for SiHA and **b** for 3T3).

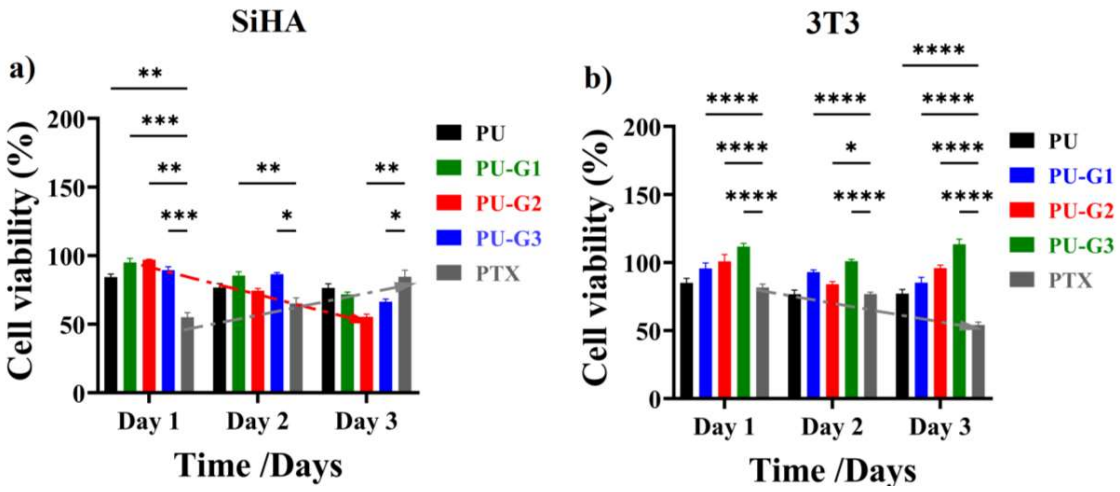

Figure 6.2.5.3: MTT assay of all the polymers assessed through cellular studies, a) *In vitro* cytotoxicity of pure drug and drug-loaded PUs on SiHA cells at various time intervals assessed using the MTT assay at a concentration of 20 µg/ml, b) *In-vitro* cytotoxicity of pure drug and drug-loaded PUs on 3T3 cells at different time intervals evaluated using the MTT assay at a concentration of 20 µg/ml.

Over time, the pure drug exhibits a tendency to increase cell viability (lower cell mortality); nevertheless, on day 1, the SiHA cell line showed somewhat higher cell death, perhaps as a result of being exposed to the cellular media right away. On the other hand, the 3T3 cell line showed a slow rise in cell death over time. The acidic nature, as well as the better engulfing ability of cancer cells, is responsible for the initial mortality rate. Although anticancer drugs work by inducing DNA damage, inhibiting DNA replication, or interfering with cell division[292]. Since DNA replication and cell division are not exclusive to tumor cells, these drugs affect any cell undergoing division, leading to toxicity in normal cells as well. This is where the PU-G2 (20 µg/ml) vehicle comes into play. Over the course of a three-day study, it selectively kills 54% of SiHA cells, while the drug-loaded system keeps 98% of 3T3 cells

viable at the same dosage, while it kills up to 44% of SiHA cells, leaving 94% of 3T3 cells alive (**Figure 6.2.5.4**) when the dose is increased up to 100 µg/ml. Again, PU-G3 exhibits slower drug release in comparison to PU-G2, as seen by the cumulative release rate (**Figure 6.2.4. (i)a**), making it the second-best material for this investigation.

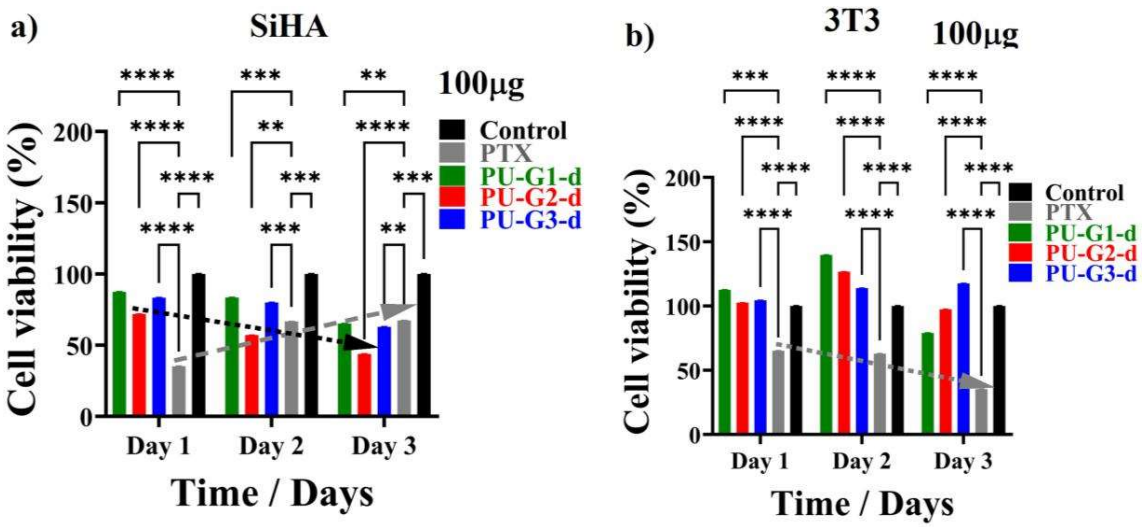

Figure 6.2.5.4: shows the biocompatibility of all the drug-loaded samples via MTT data in both SiHA and 3T3 cell lines at 100 µg concentration.

Polyurethanes were designed in such a way that they use peptides to bind and recognize particular antigens or receptors that are overexpressed on the surface of tumor cells[293]. These receptors are frequently exclusive to cancer cells or are found in significantly greater concentrations than in healthy cells. These targeting peptides are integrated into the polymer structure to enable the delivery vehicle to precisely target tumor cells. The drug is protected by the polymer, which also helps to regulate the drug's delivery by preventing it from degrading outside the cellular environment. The polymer can be made to react to particular stimuli in the tumor microenvironment (hypoxia and acidity trigger stress responses), including low pH or particular enzymes, so that it only releases the drug in the area around.

Again, malignant cells use (matrix metalloproteinases)[294] MMPs to degrade the extracellular matrix, facilitating easier molecular penetration. Hypoxia and acidic conditions[295] force these cells to adapt by increasing endocytosis and nutrient uptake (peptide-grafted PU engulfing occurs), enabling them to meet the demands of their heightened metabolic state.

Thus, the (DDS) refers to approaches for the safe and effective transportation of pharmaceutical agents into the cell, leading to desirable therapeutic effects.

6.3 Conclusion

Peptide-based polymeric units (PUs) with favorable biocompatibility and bioavailability properties were produced using TDI as the hard segment, PTMG as the soft segment, and Gly and its homopeptides as the chain extender. The addition of chain extenders to PU is validated by NMR, FTIR, and UV, and these did not show any negative impact on SiHA or 3T3 cells. Dipeptide-grafted polyurethane (PU-G2) improved porosity, hydrophilicity, and degradation behavior relative to pure PU. This resulted in a 31% drug release (PTX) from PU-G2 over the course of 24 hours, compared to only 9% for pure PU. Notably, the release from the carrier is regulated and prolonged, concentrating on the cancer cell exclusively for a duration of three days, hence diminishing the necessity for consistent drug administration. Drug-loaded PU-G2 and PU-G3 both showed more than 90% viability at 100 µg/ml on 3T3 cells, but PU-G2 has a more beneficial drug release with more cancer cell-killing potential. So, prolonged drug release and excellent biocompatibility make the second-generation vehicle (PU-G2) a good option for use as an anti-cancer drug delivery system (which exactly follows a "Blitzkrieg" Warfare mechanism).